JPL PUBLICATION 83-72

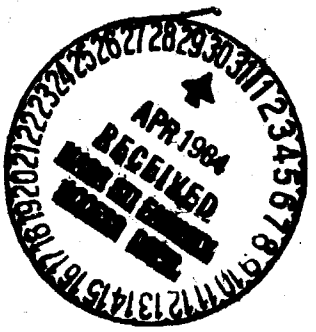

Background Sources in Optical Communications

Victor A. Vilnrotter

November 15, 1983

National Aeronautics and
Space Administration

Jet Propulsion Laboratory
California Institute of Technology
Pasadena, California

TECHNICAL REPORT STANDARD TITLE PAGE

1. Report No. 83-72	2. Government Accession No.	3. Recipient's Catalog No.
4. Title and Subtitle Background Sources in Optical Communications		5. Report Date November 15, 1983 6. Performing Organization Code
7. Author(s) Victor A. Vilnrotter		8. Performing Organization Report No.
9. Performing Organization Name and Address JET PROPULSION LABORATORY California Institute of Technology 4800 Oak Grove Drive Pasadena, California 91109		10. Work Unit No. 11. Contract or Grant No. NAS 7-100 13. Type of Report and Period Covered JPL Publication
12. Sponsoring Agency Name and Address NATIONAL AERONAUTICS AND SPACE ADMINISTRATION Washington, D.C. 20546		14. Sponsoring Agency Code RE 141 B9-310-20-67-55-00

15. Supplementary Notes

16. Abstract

This study addresses the characterization and measurement of background radiation relevant to optical communications system performance. The necessary optical receiver parameters are described, and radiometric concepts required for the calculation of collected background power are developed. The most important components of optical background power are discussed, and their contribution to the total collected background power in various communications scenarios is examined.

17. Key Words (Selected by Author(s))	18. Distribution Statement
Communications Infrared and Ultraviolet Detection Optical Detection	Unclassified - Unlimited

19. Security Classif. (of this report)	20. Security Classif. (of this page)	21. No. of Pages	22. Price
Unclassified	Unclassified	36	

JPL PUBLICATION 83-72

Background Sources in Optical Communications

Victor A. Vilnrotter

November 15, 1983

National Aeronautics and
Space Administration

Jet Propulsion Laboratory
California Institute of Technology
Pasadena, California

The research described in this publication was carried out by the Jet Propulsion Laboratory, California Institute of Technology, under contract with the National Aeronautics and Space Administration.

ABSTRACT

This study addresses the characterization and measurement of background radiation relevant to optical communications system performance. The necessary optical receiver parameters are described, and radiometric concepts required for the calculation of collected background power are developed. The most important components of optical background radiation are discussed, and their contribution to the total collected background power in various communications scenarios is examined.

ACKNOWLEDGMENT

The author wishes to thank James R. Lesh, Steven H. Pravdo, and John E. Stacey for their review of the original manuscript.

CONTENTS

Figures

CONTENTS (contd)

SECTION 1

INTRODUCTION

Background radiation collected by an optical receiver tends to impair signal detection by increasing the uncertainty associated with the message-bearing signal. Thus, optical receivers operating in high-background environments must often be designed to limit background interference, in order to achieve the desired level of performance.

The total background power collected by an optical receiver is a function of receiver parameters as well as of the characteristics of the radiating background source. Therefore, Section 2 is devoted to the definition of the basic receiver parameters that determine collected background power. Radiometric quantities generally employed for radiation measurements are defined in Section 3, while the most common sources of background radiation are examined in Section 4. Finally, Section 5 considers specific background radiation sources that may affect the performance of free-space, atmospheric, and space-to-underwater optical communications links.

SECTION 2

RELEVANT SYSTEM PARAMETERS

The amount of background radiation entering an optical receiver depends on the area of the receiving aperture $A_r(m^2)$, the receiver field of view Ω_r (sr), the spectral passband $[\lambda, \lambda + \Delta\lambda)$ (μm), and the characteristics of the radiating background environment observed by the receiver. It is convenient to associate a Cartesian coordinate system with the plane of the receiving aperture, as shown in Fig. 2-1. The receiving aperture may be viewed simply as a region of the x-y plane around the origin. In practical systems the aperture can usually be modeled as a circular region centered at the origin; however, obstructions of various kinds may also be present, particularly when reflecting components are employed. In that case A_r is taken to be the area of the unobstructed aperture. Consider the unit vector $\hat{p} \triangleq \sin\theta\cos\phi\hat{i} + \sin\theta\sin\phi\hat{j} + \cos\theta\hat{k}$, as defined in Fig. 2-1 (in which $\hat{i}$, $\hat{j}$, and $\hat{k}$ are unit vectors along the x, y, and z axes, respectively). The projected area of a planar aperture of arbitrary shape onto the plane perpendicular to $\hat{p}$ is $A_r\cos\theta$. The simplicity of the relationship between the aperture area and its projection provides the major justification for the use of a plane-aperture model. However, it must be remembered that the plane-aperture model may not be sufficiently accurate if optical surfaces or obstructions within the aperture extend significantly outside of the x-y plane. The model then has to be modified to account for these effects.

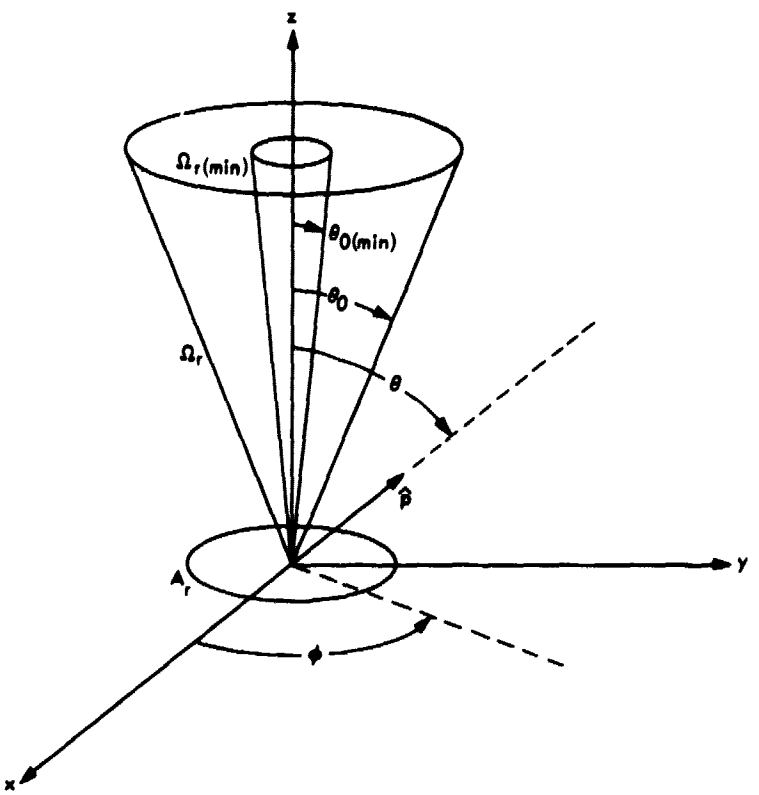

Figure 2-1. Optical receiver parameters

The receiver field of view Ω_r defines the set of directions from which radiation is accepted by the receiver. If the field of view is circularly symmetric around the z-axis, with half-cone angle θ_o, then

$$\Omega_r = 2\pi(1 - \cos\theta_o) \quad \text{sr} \tag{2-1}$$

If $\theta_o << 1$ rad, then $\cos\theta_o \simeq (1 - \frac{1}{2}\theta_o^2)$ and the approximation

$$\Omega_r \simeq \pi\theta_o^2 \quad \text{sr};\ \theta_o << 1 \text{ rad} \tag{2-2a}$$

may be used. If $\theta_o = \pi/2$ radians, then

$$\Omega_r = 2\pi \quad \text{sr};\ \theta_o = \pi/2 \text{ rad} \tag{2-2b}$$

Due to diffraction effects, receiver field of view cannot be made arbitrarily small without incurring severe losses in signal power. For an unobstructed circular aperture of area $A_r = \pi R_r^2$, designed to receive optical signals from a distant point-source located on the z-axis over an incremental bandwidth $[\lambda, \lambda + d\lambda)$, a field of view $\Omega_r \gtrsim 1.17\ \lambda^2/R_r^2 \triangleq \Omega_{r(min)}$ is required in order to collect most of the available signal power. Thus, θ_o should always exceed $\theta_{o(min)} \triangleq 0.61\ \lambda/R_r$. In free-space communications it is often desirable to operate with values of θ_o significantly greater than $\theta_{o(min)}$ in order to relax pointing requirements on the receiver. When communicating through turbulent or scattering channels that tend to increase the effective size of the signal source, $\theta_o >> \theta_{o(min)}$ may again be required to collect all of the signal power available at the receiver. Receiver field of view need not be circularly symmetric. Usually, the design goal is to limit the background power reaching the detector while collecting sufficient signal power to allow acceptable communications performance. Thus, an over-the-horizon optical receiver observing signal power scattered out of a narrow laser beam might be designed with an elongated field of view matched to the apparent dimensions of the signal beam.

Spectral filtering is generally employed in optical receivers to reduce the background power reaching the detector. If the significant spectral components of the modulated optical signal field at the receiver are contained in the wavelength range $[\lambda, \lambda + \Delta\lambda)$, then ideally the receiver should be designed to accept radiation only within this bandwidth. In real systems filter functions may deviate significantly from the ideal, and in addition may depend on the arrival angle of the impinging radiation. In that case, each incremental received power must be multiplied by the proper wavelength and angle-dependent weighting factor to account for these effects.

SECTION 3

MEASUREMENT OF BACKGROUND RADIATION

Background radiation is the result of spontaneous emission from sources at a high temperature, reflection of thermal radiation from cooler surfaces, or a combination of both mechanisms. The spectral radiant emissivity of a source is defined as the ratio of the spectral radiant power per unit area emitted by the source to the spectral radiant power per unit area for a blackbody at the same temperature. In general, the spectral radiant emissivity of a substance depends on both wavelength and temperature. Given an accurate model for the spectral radiant emissivity of a source, its spectral radiant emittance can be found in terms of that of a blackbody at the same temperature. This latter quantity can be determined using Planck's law of blackbody radiation, according to which the unpolarized power emitted per unit area of the source into a hemisphere, in the incremental wavelength range $[\lambda, \lambda + d\lambda)$, is

$$W(\lambda)d\lambda = \left(\frac{2\pi c^2 h}{\lambda^5}\right) \frac{d\lambda}{[\exp(hc/\lambda kT) - 1]} \quad \text{watts/cm}^2 \qquad (3\text{-}1)$$

Here $W(\lambda)$ is the spectral radiant emittance of the blackbody, c is the velocity of light, λ is the wavelength, T is the temperature of the blackbody, h is Planck's constant, and k is Boltzmann's constant (Refs. 1 and 2). The spectral radiant emittance of a blackbody radiator is shown in Fig. 3-1 as a function of wavelength for various temperatures. A source whose spectral radiant emissivity is not unity is called a graybody. At a given temperature, the spectral radiant emittance of a graybody can be expressed as the product of its spectral radiant emissivity and the spectral radiant emittance of a blackbody at the same temperature.

Consider a flat surface radiating as a blackbody. When observed from an angle θ_s from the surface normal, the projected area of a differential surface element is $dA_s \cos\theta_s$. Define the spectral radiance of the surface as the power radiated into a unit solid angle per unit bandwidth and unit projected area. For a Lambertian (diffuse) surface, the spectral radiance is independent of direction. Denoting this spectral radiance by $N(\lambda)$, the incremental power dP_s radiated into an infinitesimal solid angle $d\omega_s$ at an angle θ_s from the surface normal, from the differential surface element dA_s over the wavelength range $[\lambda, \lambda + d\lambda)$, is (Ref. 2)

$$dP_s = N(\lambda)dA_s \cos\theta_s d\omega_s d\lambda \quad \text{watts} \qquad (3\text{-}2)$$

Integration over the hemisphere yields

$$dP_s = \pi N(\lambda)dA_s d\lambda \quad \text{watts} \qquad (3\text{-}3)$$

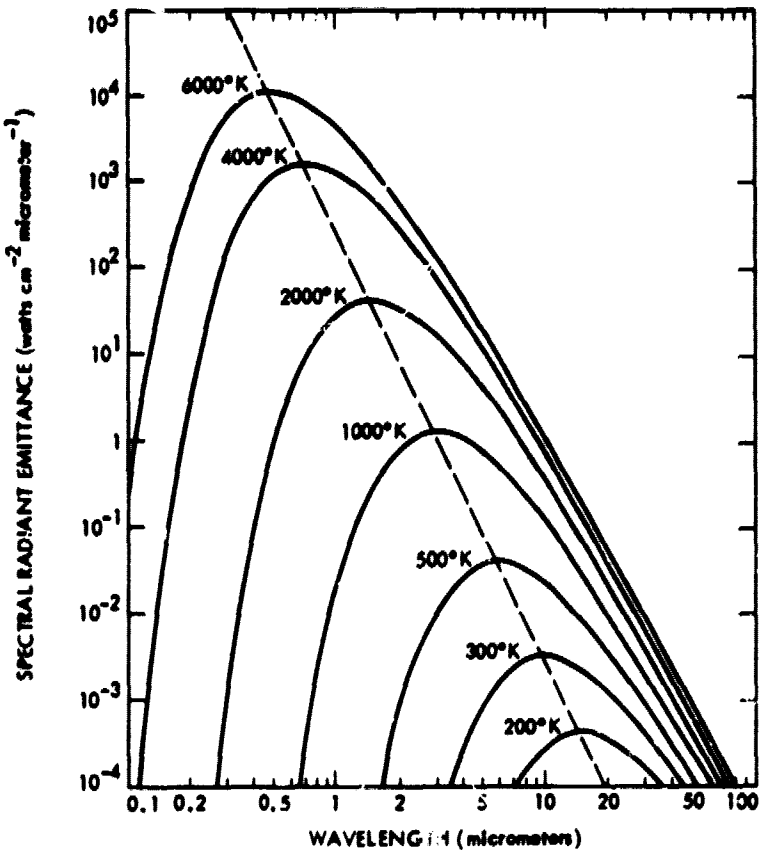

Figure 3-1. Spectral radiant emittance of a blackbody as a function of wavelength for various temperatures (Ref. 2)

Since $dP_s = W(\lambda)dA_s d\lambda$, it follows that for a Lambertian surface

$$N(\lambda) = W(\lambda)/\pi \qquad \text{watts/cm}^2\text{-}\mu\text{m-sr} \tag{3-4}$$

The amount of power collected by an optical receiver from a radiating Lambertian surface a great distance from the receiver can be found by means of equation (3-2). Let the distance between the receiving aperture and the source be L, where L is much greater than the maximum linear dimensions of the receiving aperture. From Fig. 3-2, a differential receiver field of view $d\Omega_r = \sin\theta\, d\theta\, d\phi$ observes a differential surface element on the source $dA_s = d\Omega_r L^2/\cos\theta_s$, where θ_s is the angle between the surface normal and the line of sight. Viewed from this surface element, the receiver subtends an approximate solid angle $(A_r \cos\theta)/L^2$. The spectral radiance of the source may not be constant over the entire surface, in which case it can be represented as $N(\lambda;\theta,\phi)$ where θ and ϕ are the line-of-sight coordinates of a differential receiver field of view, as in Fig. 3-2. Hence, the incremental received power dP_r over the differential wavelength range $[\lambda, \lambda + d\lambda)$ is

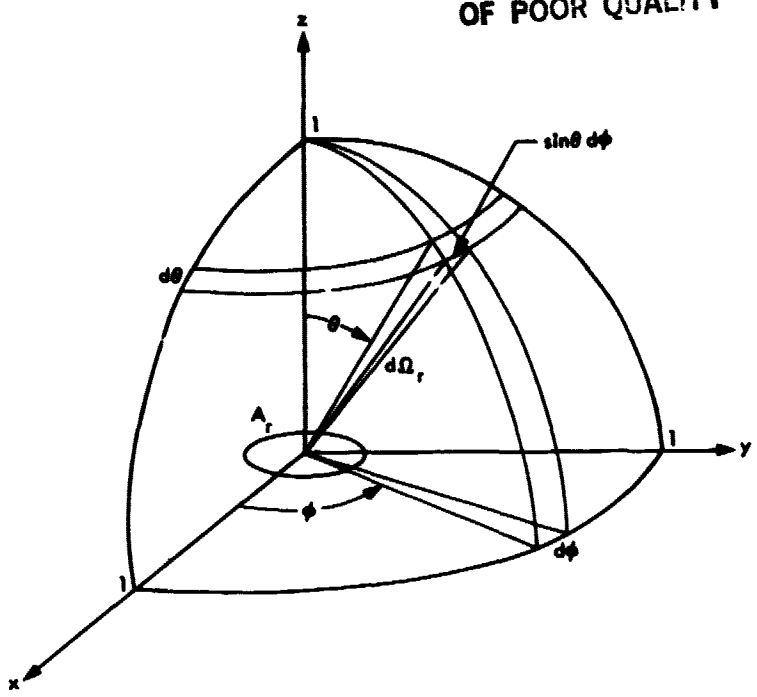

Figure 3-2. Receiver plane with associated Cartesian and spherical coordinate systems

$$dP_r = (N(\lambda;\theta,\phi)dA_s\cos\theta_s A_r\cos\theta d\lambda)/L^2$$

$$= N(\lambda;\theta,\phi)A_r\cos\theta d\Omega_r d\lambda \qquad \text{watts} \qquad (3\text{-}5)$$

Thus, for a Lambertian radiator, the incremental received power over a differential bandwidth depends only on $N(\lambda;\theta,\phi)$ and on the receiver parameters A_r, θ, and $d\Omega_r$. The total received power in $[\lambda,\lambda + \Delta\lambda)$ is simply

$$P_r = A_r \int_{\lambda}^{\lambda+\Delta\lambda} d\lambda \int_{\text{source}} d\Omega_r N(\lambda;\theta,\phi)\cos\theta \qquad \text{watts} \qquad (3\text{-}6)$$

It is useful to interpret equation (3-5) in the following way. Given an incremental received power component flowing into a differential field of view over a differential bandwidth from a particular direction (θ,ϕ), a spectral radiance function can be defined regardless of the physical characteristics of the source. For example, power scattered into the receiver from an extended scattering volume may be characterized in terms of a spectral radiance function $N(\lambda;\theta,\phi)$. This interpretation can be used to model scattered sunlight viewed by an optical receiver operating in atmospheric or underwater environments.

Spectral irradiance is the power incident on a surface per unit area and unit bandwidth. For a source distribution defined over the entire hemisphere, the spectral irradiance $H(\lambda)$ becomes (Ref. 3)

$$H(\lambda) = \int_0^{2\pi} d\phi \int_0^{\pi/2} d\theta N(\lambda;\theta,\phi)\cos\theta\sin\theta \qquad \text{watts/cm}^2\text{-}\mu\text{m} \qquad (3\text{-}7)$$

If a source of small angular extent is located on axis a great distance from the receiver plane, and if $N(\lambda;\theta,\phi) = N(\lambda)$, then equation (3-7) can be approximated by

$$H(\lambda) \simeq \Omega_s N(\lambda) \qquad \text{watts/cm}^2\text{-}\mu\text{m} \qquad (3\text{-}8)$$

where Ω_s is the (small) solid angle subtended by the source at the receiver. Radiation from a distant "point" source (such as a star) is generally characterized in terms of spectral irradiance. Implicit in this characterization is the assumption that the source is located on the receiver axis, so that spatial filtering by the aperture can be ignored.

Using equations (3-6) and (3-8), the total background power due to an extended background source described by $N(\lambda;\theta,\phi)$ and to K remote point sources entirely within the receiver field of view, entering a receiver with circular field of view (half-cone angle θ_o), over the bandwidth $[\lambda,\lambda+\Delta\lambda)$, becomes

$$P_r = A_r \int_\lambda^{\lambda+\Delta\lambda} d\lambda \left\{ \int_0^{2\pi} d\phi \int_0^{\theta_o} d\theta N(\lambda;\theta,\phi)\cos\theta\sin\theta + \sum_{i=1}^{K} H_i(\lambda)\cos\theta_i \right\} \qquad \text{watts} \qquad (3\text{-}9)$$

where $H_i(\lambda)$ is the spectral irradiance of the i-th point source, at an angle of θ_i radians from the normal to the receiver aperture.

In the absence of discrete background sources, and for constant spectral radiance $N(\lambda)$, equation (3-9) reduces to

$$P_r = \pi A_r N(\bar{\lambda}) \Delta\lambda \sin^2\theta_o \qquad \text{watts} \qquad (3\text{-}10)$$

where $\bar{\lambda}$ is a wavelength in $[\lambda, \lambda + \Delta\lambda)$ such that

$$N(\bar{\lambda})\Delta\lambda = \int_{\lambda}^{\lambda+\Delta\lambda} N(\lambda)\, d\lambda.$$

If, in addition, $\theta_o << 1$ so that $\sin\theta_o \simeq \theta_o$, then

$$P_r \simeq \pi A_r N(\bar{\lambda}) \Delta\lambda \theta_o^2 \qquad \text{watts;}\ \theta_o << 1 \text{ rad} \qquad (3\text{-}11a)$$

while for hemispherical field of view

$$P_r = \pi A_r N(\bar{\lambda}) \Delta\lambda \qquad \text{watts;}\ \theta_o = \pi/2 \text{ rad} \qquad (3\text{-}11b)$$

Equation (3-11a) is the usual approximation employed for narrow-field-of-view optical receivers observing an extended constant background source, whereas (3-11b) represents the total power flowing into a hemispherical field of view, taking into account spatial filtering by the planar receiving aperture.

SECTION 4

SOURCES OF BACKGROUND RADIATION

Background radiation in the terrestrial and near-earth environment is due to direct, reflected, or scattered sunlight, thermal emission from the earth, moon, and planets, starlight, zodiacal light, galactic light, auroral displays, airglow, direct and scattered artificial light, bioluminescence, and radiation of cataclysmic origins such as lightning discharges and meteor trails. In the following section the major components of background radiation are examined.

4.1 THE SUN AND STARS

Outside the terrestrial atmosphere, the spectral irradiance of the sun is similar to the radiation generated by a 5900°K blackbody, as can be seen in Fig. 4-1. At sea level, the solar spectral irradiance is attenuated due to wavelength-selective absorption by ozone, oxygen, water molecules, and carbon dioxide. Since the sun is nearly a Lambertian radiator subtending a solid angle of 6.78×10^{-5} sr at the earth, its spectral radiance can be approximated using equation (3-8); $N_{sun}(\lambda) \approx H_{sun}(\lambda)/(6.78 \times 10^{-5})$ watts/cm^2-μm-sr. Figure 4-2 shows the spectral irradiance of the brightest stars, viewed from above the terrestrial atmosphere.

4.2 THE EARTH, MOON, AND PLANETS

The spectral irradiance of the moon and planets consists of two components, one due to reflected solar radiation and the other due to self-emission.

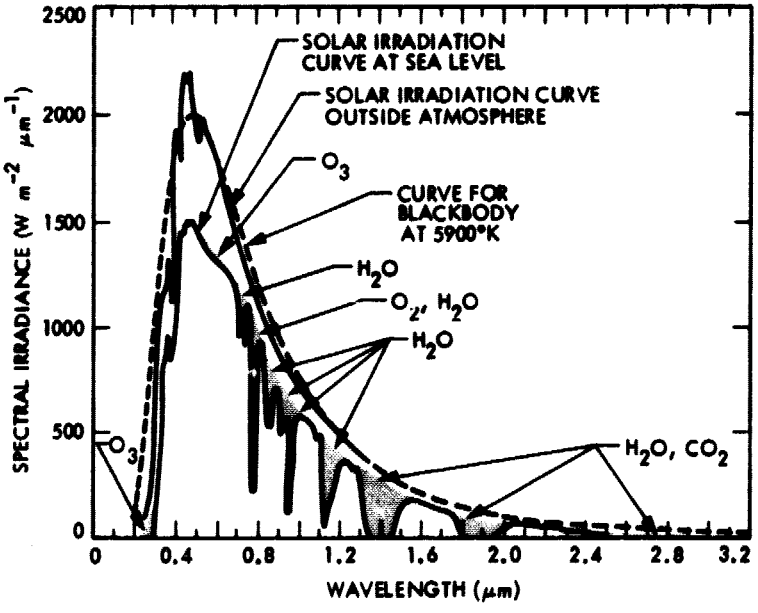

Figure 4-1. Solar spectral irradiance with the sun at zenith. Absorption bands are shown shaded (Ref. 4).

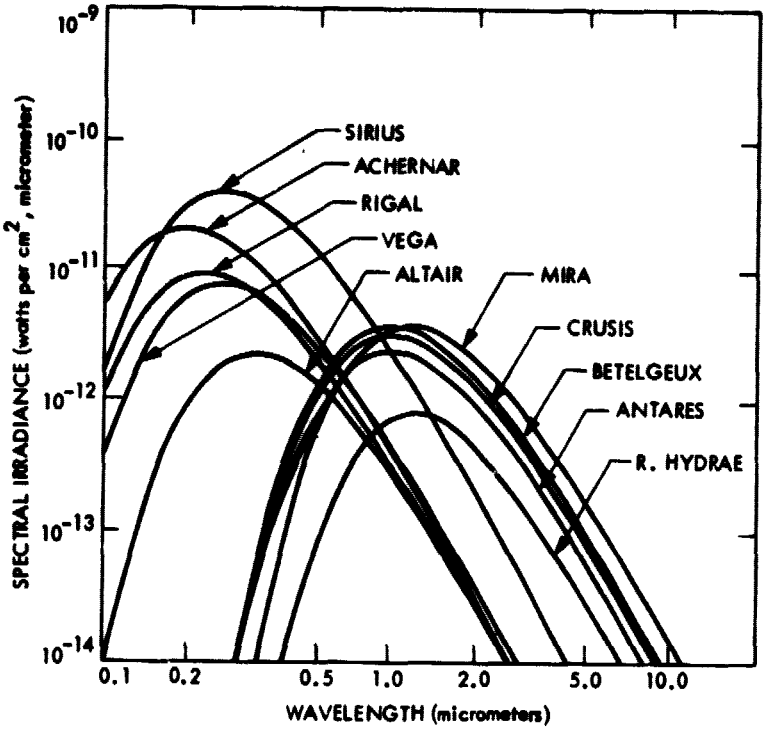

Figure 4-2. Spectral irradiance of the brightest stars viewed from outside the terrestrial atmosphere (after Ramsey, Ref. 5)

Typical irradiance curves outside the atmosphere for the full moon and the major planets are shown in Fig. 4-3, calculated for the indicated celestial geometries. These curves do not consider the variation of albedo with wavelength, hence must be modified if more accurate results are desired (Ref. 1).

The earth, when viewed from space, also appears as a source of both reflected and emitted radiation. A typical spectral radiant emittance curve for the earth, assuming no clouds, is shown in Fig. 4-4. Of course, the spectral radiance depends on the nature of the terrain being viewed. Figures 4-5a through 4-5d show characteristic calculated spectral radiance functions, at the top of a plane-parallel atmosphere, for a low-altitude cloud deck, vegetation, winter snow and ice, and soil and rocks. Elevation scans across mountainous terrain indicate considerable variation with wavelength, as can be seen in Figs. 4-6a and 4-6b.

4.3 THE SKY

Sky radiation is caused by the scattering of solar radiation and by emission from atmospheric constituents. The scattered component of sky radiance is significant only in the visible and near-infrared regions of the spectrum, and

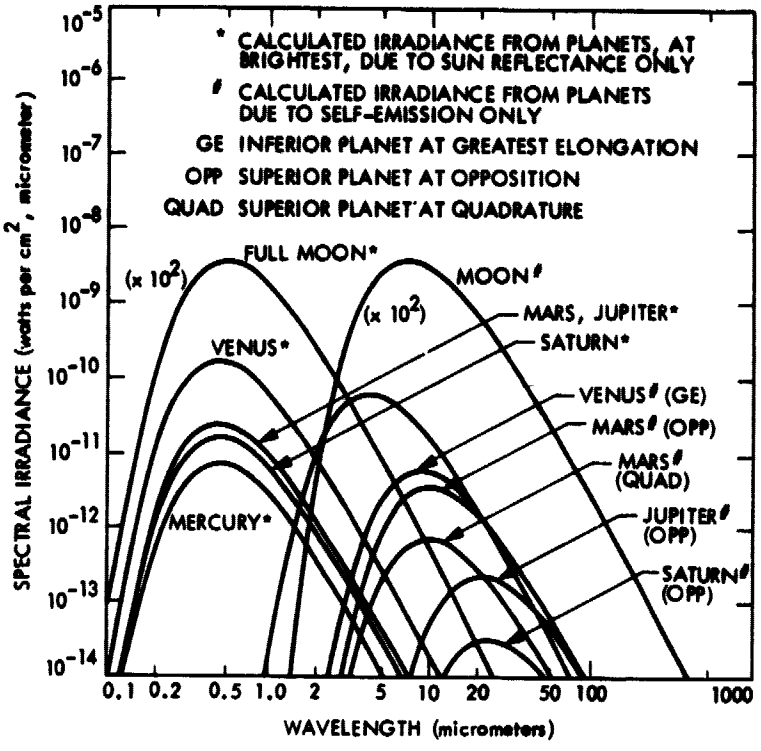

Figure 4-3. Calculated planetary and lunar spectral irradiance outside the terrestrial atmosphere (Ref. 5)

is present only during the day. Radiance due to self-emission is ever present, resembling somewhat the spectral radiance of a 300°K blackbody. The radiance of sunlit clouds is typically an order of magnitude greater than the corresponding value for clear sky. However, there is a great deal of variation in the scattered radiance for different types of clouds, depending also on factors such as sun position and direction of observation. Idealized spectral radiance functions for the sun, clear sky, clouds, and the emitting atmosphere are presented in Fig. 4-7.

The spectral radiance of the sky generally depends on visibility, elevation, and the relative position of the sun. The dependence on elevation is illustrated in Fig. 4-8, which shows the spectral radiance of clear sky at Cocoa Beach, Florida, as a function of elevation at a wavelength of 1.13 μm.

4.4 OTHER SOURCES

Other sources of background radiation at night include zodiacal light, galactic light, and scattered starlight (Fig. 4-9). In addition, direct and scattered light from artificial sources near major population centers, scattered moonlight, auroral displays, and airglow may contribute to the radiance of the night sky.

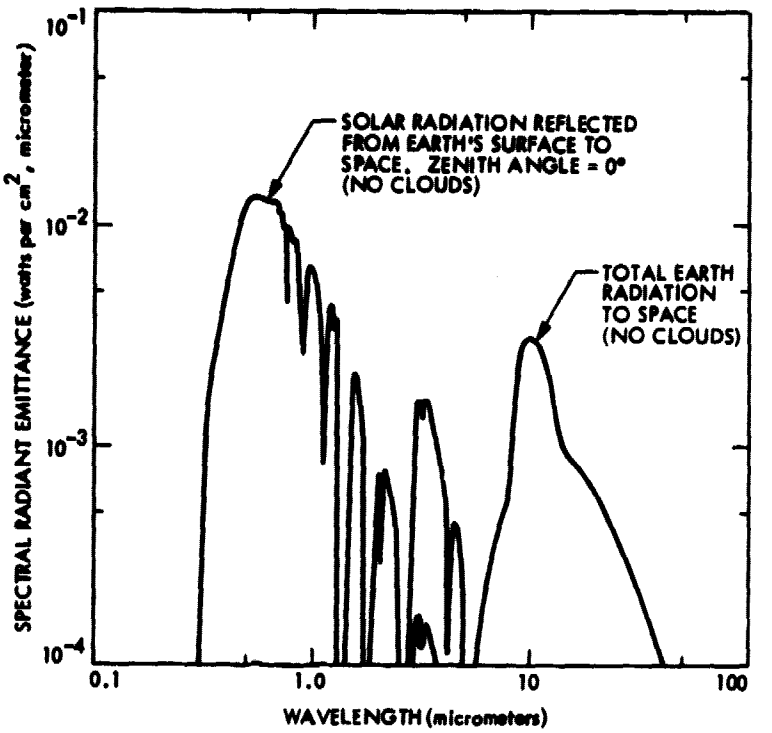

Figure 4-4. Spectral radiant emittance of the earth (Ref. 6)

In the underwater channel, scattered sunlight, skylight, and bioluminescence are the principal sources of visible radiation. Figure 4-10 shows the relative downwelling radiance in an underwater environment in the vertical plane of the sun, as a function of zenith angle, for various depths. Note that the angular distribution of radiation originating from a source of small angular extent (the sun, at a refracted zenith angle of 21°30') tends to increase with increasing depth. Calculated curves of downwelling spectral irradiance (as defined in equation (3-7)) are shown in Fig. 4-11 for Crater Lake, demonstrating the filtering effect of pure natural water. Different types and concentrations of impurities tend to alter the characteristics of spectral irradiance in oceanic waters. In the ocean, below some intermediate depth (roughly 500 m), bioluminescence begins to exceed the level of penetrating daylight at noon, even in the clearest oceanic waters (Fig. 4-12). At night, near the surface, scattered light from the moon and night sky may contribute to the total downwelling irradiance.

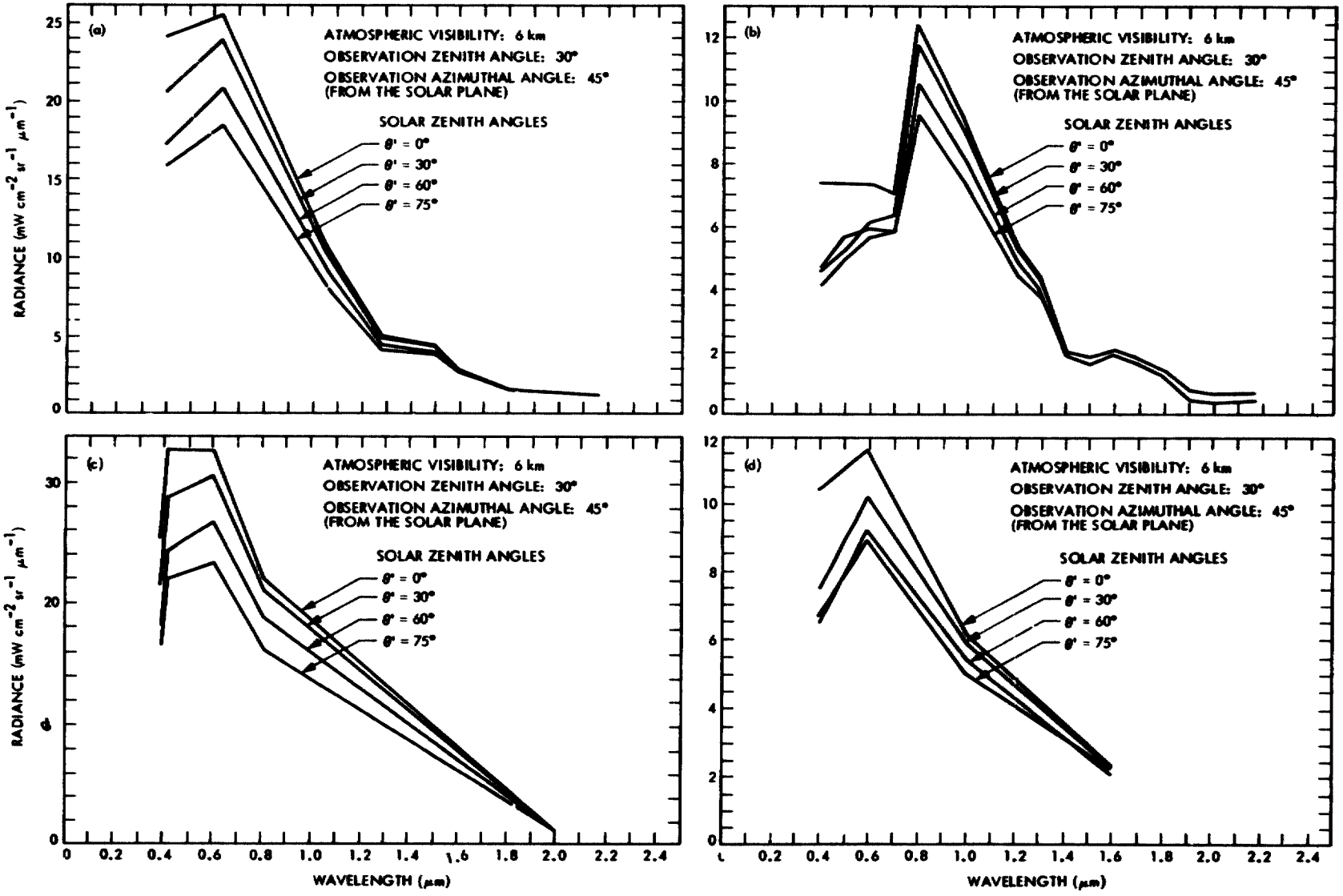

Figure 4-5. Upwelling spectral radiance of natural terrain observed at the top of a plane-parallel atmosphere (Ref. 7)
a) With the earth's surface obscured by a low-altitude cloud deck
b) With the earth's surface composed of vegetation
c) With the earth's surface composed of winter snow and ice
d) With the earth's surface composed of soil and rocks

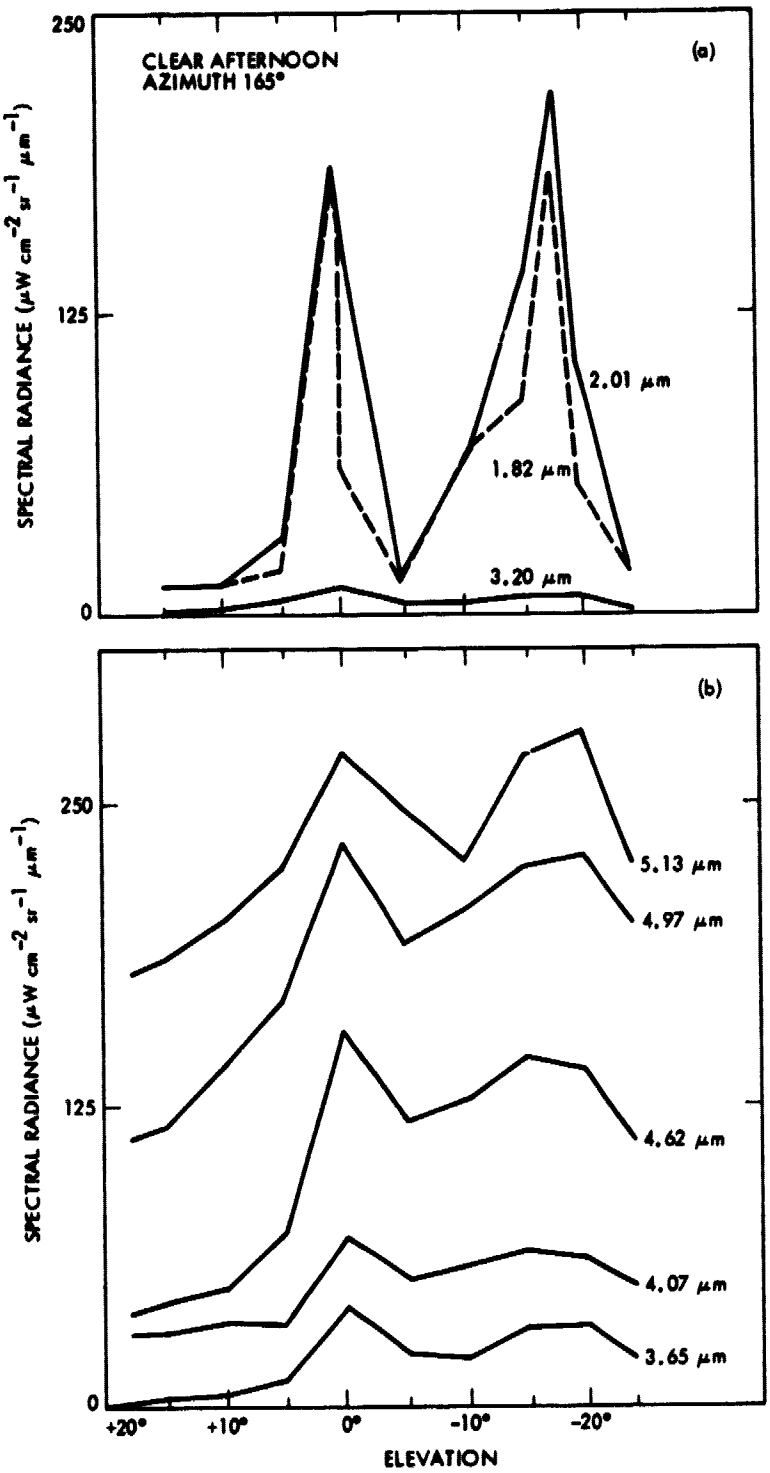

Figure 4-6. Elevation scans of spectral radiance across mountainous terrain (Ref. 8)

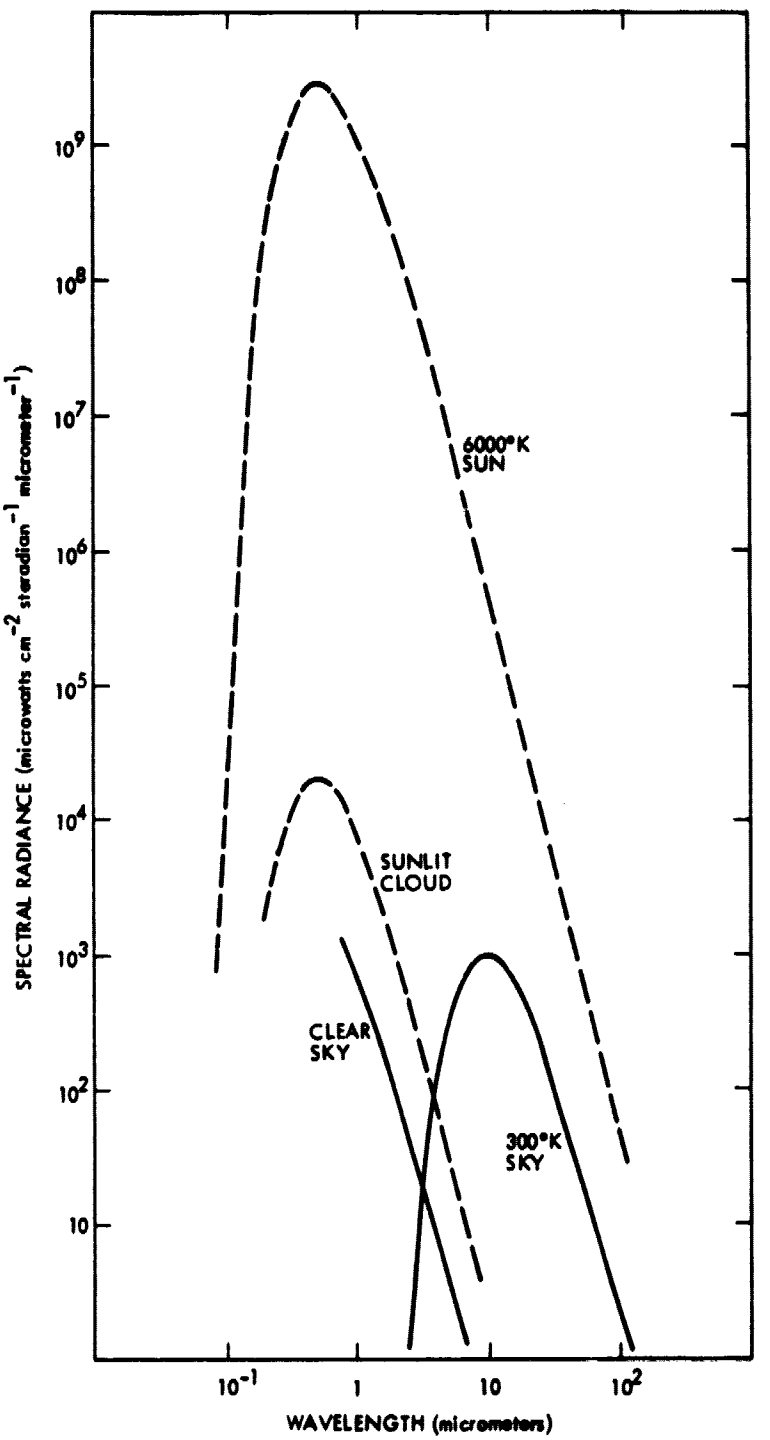

Figure 4-7. Idealized spectral radiance of the sun, the emitting atmosphere, sunlit cloud, and sunlight-scattering clear sky (Ref. 9)

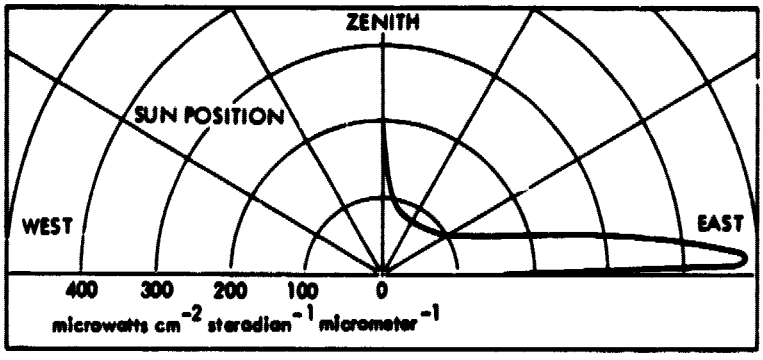

Figure 4-8. Spectral radiance of clear sky at Cocoa Beach, Florida, showing elevation-angle dependence of scattered radiation at a wavelength of 1.13 μm (Ref. 9)

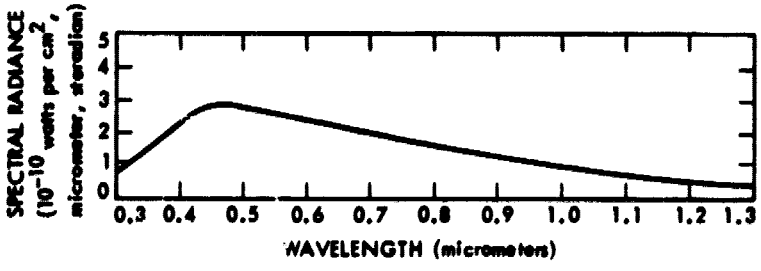

Figure 4-9. Nighttime sky radiance from zenith due to zodiacal light, galactic light, and scattered starlight (Ref. 1)

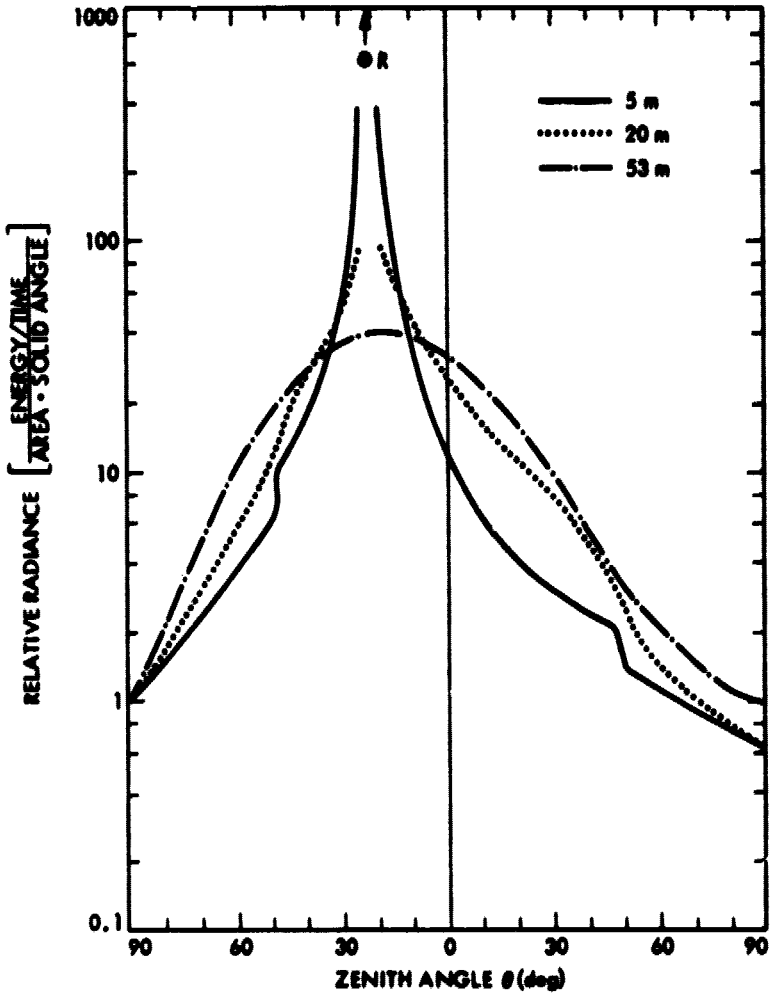

Figure 4-10. Relative radiance versus zenith angle for downwelling radiance in the vertical plane of the sun. The curves have been arbitrarily normalized to unity at $\theta = 90°$ so that they may be readily compared. Other information: zenith angle of the sun 28°, refracted angle of the sun 21°30', clear skies (less than 0.1 cloud cover), moderate breeze (Beaufort No. 4) with gusts to 25 knots, wind-chopped moderate sea (1 to 1-1/2 m waves) in lee of island, instrument suspended 4 m from stern of ship (R/V Ellen B. Scripps), and 60-nm-bandwidth (FWHM) spectral response approximately centered at the wavelength of maximum transmittance of the water under investigation (λ max. $\approx$ 497 nm obtained using Wratten No. 64 filter). Gulf of California (Fresnel II Cruise-Sta. 2) 16 March 1971, 25°26' N 111°08' W (Ref. 10).

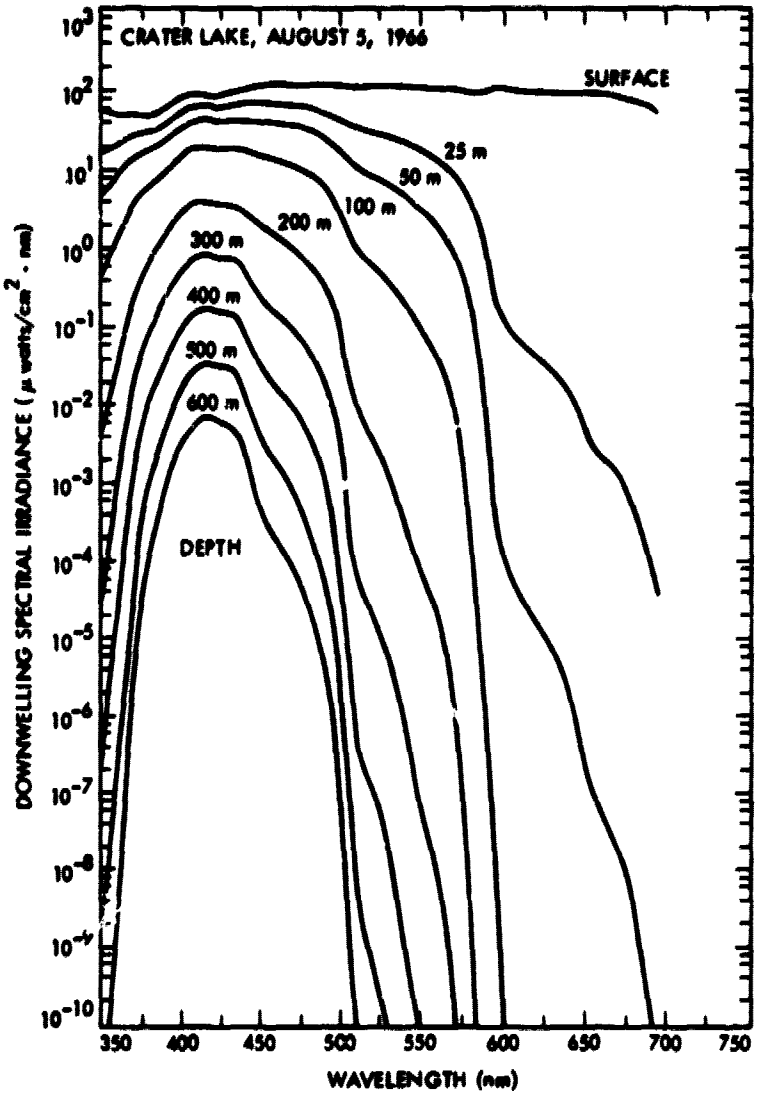

Figure 4-11. Calculated daytime downwelling spectral irradiance for Crater Lake, obtained from measured spectral irradiance at 10 m and using average values of spectral diffuse attenuation coefficients (Ref. 11)

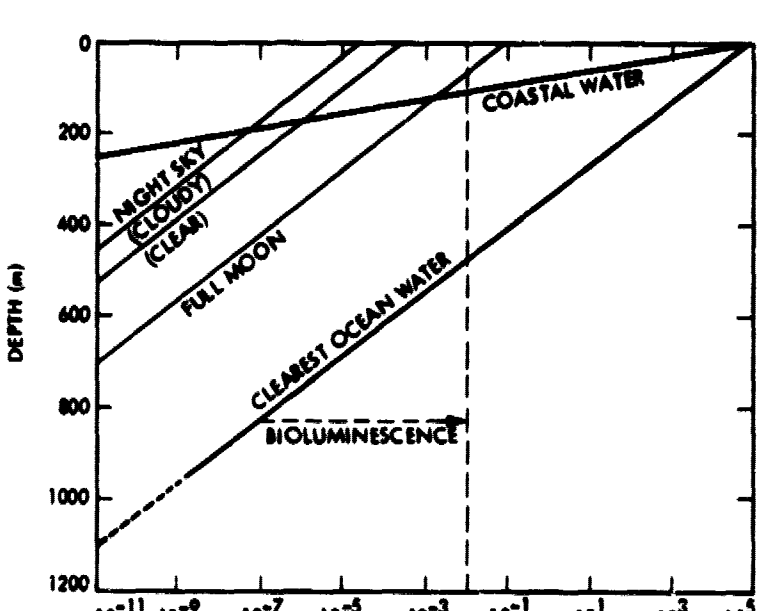

Figure 4-12. Downwelling irradiance as a function of depth in the sea (after Clarke, Ref. 12). The heavy solid lines indicate the penetration of sunlight into oceanic waters, while the lighter solid lines indicate the downwelling underwater irradiance at night.

SECTION 5

BACKGROUND RADIATION IN OPTICAL COMMUNICATIONS LINKS

In this section, background radiation sources relevant to various optical communications scenarios are examined. In particular, free-space links, atmospheric links, and space-to-underwater links are considered.

5.1 FREE-SPACE LINKS

This category includes communications links between earth-orbiting satellites or satellites and deep-space vehicles. The major sources of background radiation in the free-space channel are direct and reflected sunlight, self-emission from the earth, moon and planets, and direct radiation from stars. Sunlight reflected directly from the transmitter may contribute to the total background power. When communicating between a satellite transmitter in low earth orbit and a receiver in higher orbit, reflected sunlight from the earth may enter the receiver field of view. In that case, the received background power depends on the type of terrain viewed by the receiver, and spectral-radiance curves such as those in Fig. 4-5 can be used to assess the total instantaneous collected power. Theoretically, free-space receivers could operate with essentially diffraction-limited fields of view, provided the tracking requirements can be accommodated. In practice, it may be necessary to operate with much greater than diffraction-limited, but still narrow, fields of view. Since the transmitter may be in motion with respect to the background, the background power collected by the receiver can vary rapidly as terrains (or other background sources) with different characteristics are observed. In general, the actual received power depends on orbital geometry and on the location of the sun.

When a low-orbiting receiver views a transmitter in a higher orbit, the sun, stars, planets, moon, zodiacal light, and possible transmitter-reflected sunlight contribute to the total background power. Again, temporal variation of background power may occur due to apparent motion of the background as the transmitter is tracked.

For narrow-field-of-view receivers ($\theta_o << 1$ rad) operating in the free-space environment, the instantaneous background power through a receiver aperture A_r over a given narrow wavelength range $[\lambda, \lambda + \Delta\lambda)$ can be obtained using equation (3-9). The amount of background radiation per unit bandwidth collected by a 100-cm^2 receiver aperture at a mean wavelength of 1 μm is shown in Fig. 5-1 as a function of θ_o for the sun, some representative stars, and various terrains. The power contribution of each star is essentially independent of θ_o for $\theta_o > \theta_o(\text{min})$, although a greater number of stars are likely to be observed as the field of view is increased.

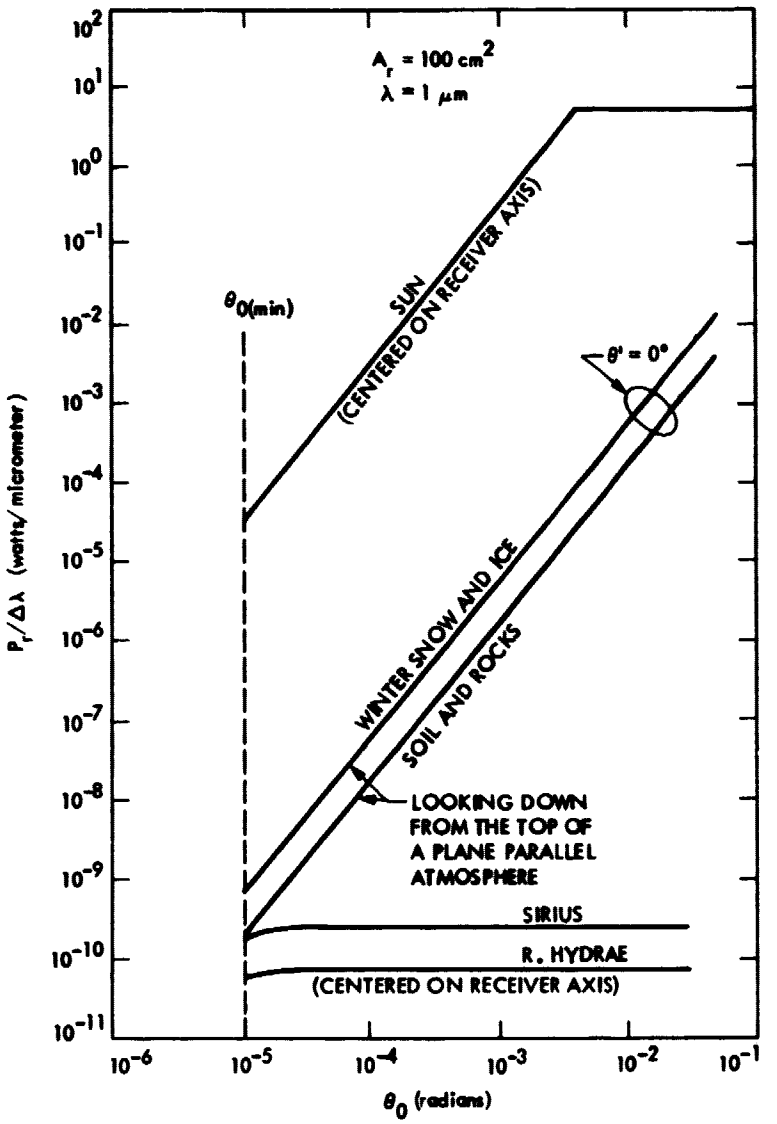

Figure 5-1. Received power per unit wavelength (free-space channel)

5.2 ATMOSPHERIC LINKS

Here we consider examples where a significant part of the communications link is immersed in the terrestrial atmosphere. Airplane-to-airplane, airplane-to-ground and satellite-to-ground links fall under this category. In atmospheric communications systems diffraction-limited fields of view can only be used with small-aperture receivers, due to the limitations imposed by atmospheric turbulence. (Under good conditions, $\theta_o \gtrsim 5 \times 10^{-6}$ rad is required).

Heat generated by aircraft engines can be a source of background radiation in the infrared region of the spectrum. Temporal variation in background power can occur if the transmitter aircraft passes in front of small sunlit clouds or illuminated natural terrain. A high-flying aircraft or satellite viewing a stationary source on the ground tends to observe only a fixed region around the transmitter; hence, only slow variation in background (due to changing link geometry) would be expected. On a clear day, a stationary receiver on the ground tracking a high-flying transmitter (aircraft or satellite) would observe only slowly varying sky radiance, but might encounter rapidly changing starfields at night. However, as shown in Fig. 5-1, starlight passing through a narrowband filter typically represents very weak background radiation, even above the terrestrial atmosphere. The background power per unit wavelength passing through a 100-cm^2 aperture at a wavelength of 1 μm is shown in Fig. 5-2 as a function of θ_o, in the range $5 \times 10^{-6} \leq \theta_o \leq 0.1$ rad, for clear sky and sunlit clouds. In the atmosphere, reception through haze, fog, or light clouds may require wide-field-of-view receivers. An estimate of the actual power levels for various filter bandwidths can be obtained using the curves in Fig. 5-2, or similar data.

5.3 SPACE-TO-UNDERWATER LINKS

When receiving optical fields at a submerged platform, the severe scattering properties of water must be taken into account. At great depths, receivers with hemispherical fields of view may be required to collect all of the available signal power. In addition, such receivers also collect background power from all directions, consisting mainly of scattered sunlight and, in the ocean, bioluminescence. The amount of scattered sunlight collected by a receiver with a hemispherical field of view over a wavelength range $[\lambda, \lambda + \Delta\lambda)$ can be calculated using underwater spectral irradiance data such as that shown in Fig. 4-11. As an example, Fig. 5-3 was prepared using the data of Fig. 4-11. It shows the scattered sunlight collected by a 100-cm^2 receiver aperture pointed towards the zenith at a wavelength of 425 nm, as a function of depth The spectral irradiance function was assumed constant over bandwidths of 100 A or less. Due to impurities, spectral irradiance functions for other bodies of water may differ significantly from those of Fig. 4-11. To obtain accurate background-power levels for other locales, spectral irradiance functions characteristic of the particular environment should be employed.

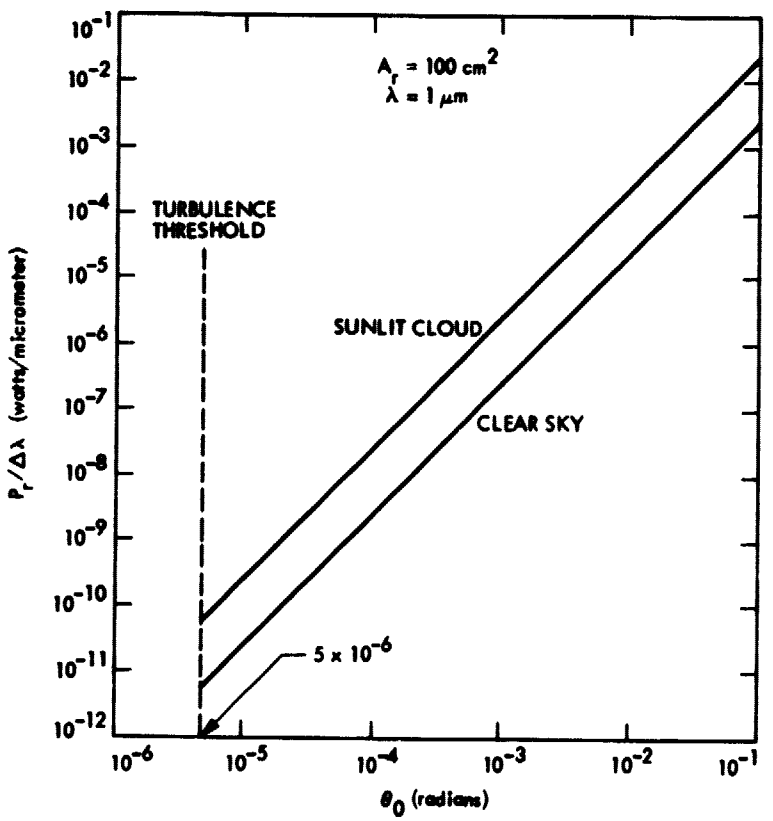

Figure 5-2. Received power per unit wavelength (atmospheric channel)

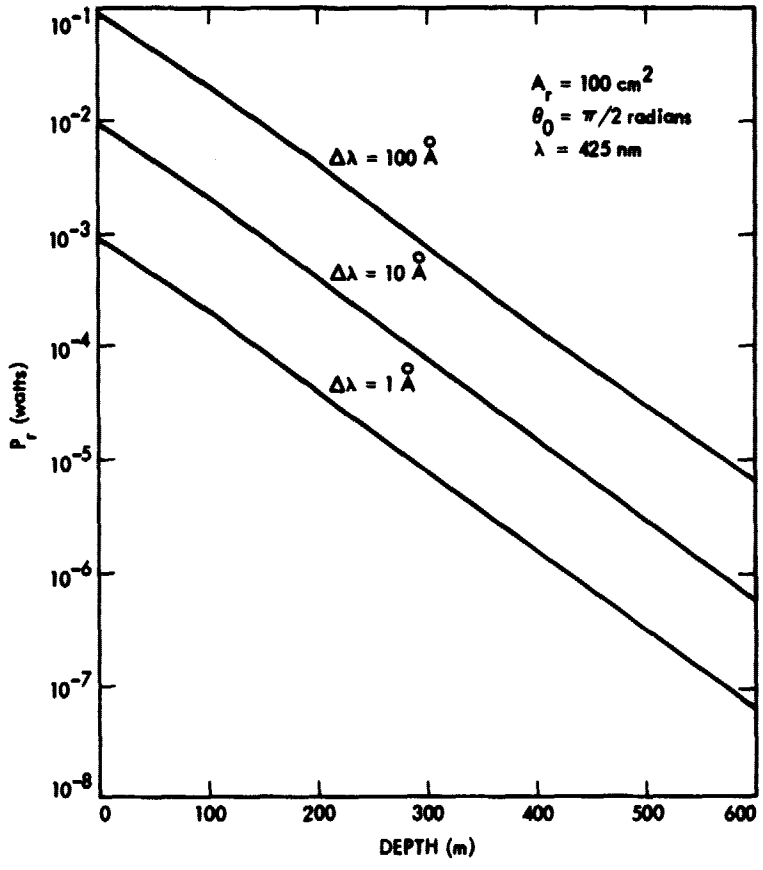

Figure 5-3. Scattered sunlight collected by submerged aperture, hemispherical field of view, Crater Lake data

REFERENCES

1. Pratt, W. K., Laser Communications Systems, John Wiley and Sons, New York, 1969, Chapt. 6.

2. Jamieson, J. A., McFee, R. H., Plass, G. N., Grube, R. H., and Richards, R. G., Infrared Physics and Engineering, McGraw-Hill, New York, 1963, Chapt. 2.

3. Nicodemus, F. E., Self-Study Manual on Optical Radiation Measurements: Part I - Concepts, National Bureau of Standards Technical Note 910-2, 1978, Chapt. 4.

4. Wolfe, W. L. and Zissis, G. J., The Infrared Handbook, Environmental Research Institute of Michigan, Office of Naval Research, Department of the Navy, Washington, D.C., 1978, Chapt. 3.

5. Ramsey, R. C., "Spectral Irradiance from Stars and Planets, Above the Atmosphere, from 0.1 to 100 Microns", Applied Optics, Vol. 1, No. 4, July 1962, pp. 465-471.

6. Goldberg, I. L., Radiation from Planet Earth, U.S. Army Signal Research and Development Laboratory, Report 2231, AD-266-790, Sept. 1961.

7. Rose, H., et al., The Handbook of Albedo and Thermal Earthshine, Environmental Research Institute of Michigan, Ann Arbor, MI, Report No. 190201-1-T, 1973.

8. Bell, E. E., Eisner, L., Young, J., and Oetjen, R. A., "Spectral Radiance of Sky and Terrain at Wavelengths between 1 and 20 microns. III. Terrain Measurements", JOSA, Vol. 52, No. 2, pp. 201-209.

9. Bell, E. E., Eisner, L., Young, J., and Oetjen, R. A., "Spectral Radiance of Sky and Terrain at Wavelengths between 1 and 20 microns. II. Sky Measurements", JOSA, Vol. 50, No. 12, pp. 1313-1320.

10. Jerlov, N. G. and Nielsen, E. S., Optical Aspects of Oceanography, Academic Press, New York, 1974, Chapt. 5.

11. Tyler, E. J. and Smith, R. C., Measurement of Spectral Irradiance Underwater, Gordon and Breach, New York, 1970, Chapt. 5.

12. Clarke, G. L., in Proceedings of the International Symposium on Biological Sound Scattering in the Ocean, 1970 (G. B. Farquhar, ed.), Maury Center for Ocean Science, Department of the Navy, Washington, D.C., pp. 41-50.